Interaction of long-chain nicotinates with dipalmitoylphosphatidylcholine

Hans-Joachim Lehmler,[1,*] Azarih Fortis-Santiago,[*] Dhananjaya Nauduri,[*] and Paul M. Bummer[†]

Department of Occupational and Environmental Health,* University of Iowa, Iowa City, IA 52242; and College of Pharmacy,† University of Kentucky, Lexington, KY 40536

Abstract The interaction of four long-chain nicotinates, compounds that are of interest as potential chemopreventive agents, with dipalmitoylphosphatidylcholine (DPPC) was investigated in monolayers at the air-water interface and in fully hydrated bilayers. For the monolayer studies, the compression isotherms of mixtures of the respective nicotinate with DPPC were recorded at various compositions on a hydrochloric acid subphase (pH 1.9–2.1, 37 ± 2°C). The headgroup of the nicotinates (24–29 Å^2/molecule) is larger than that of the hydrophobic tail (20 Å^2/molecule). The pure nicotinates exhibit a temperature- and chain length-dependent transition from an expanded to a condensed phase. Analysis of the concentration dependence of the average molecular area at constant film pressure and the concentration dependence of the breakpoint of the phase transition from the expanded to the condensed state suggests that all four DPPC-nicotinate mixtures are partially miscible at the air-water interface. Although a complex phase behavior with several phase transitions was observed, differential scanning calorimetry studies of the four mixtures are also indicative of the partial miscibility of DPPC and the respective nicotinate. Overall, the complex phase behavior most likely results from the head-tail mismatch of the nicotinates and the geometric packing constraints in the two-component lipid bilayer.—Lehmler, H-J., A. Fortis-Santiago, D. Nauduri, and P. M. Bummer. **Interaction of long-chain nicotinates with dipalmitoylphosphatidylcholine.** ***J. Lipid Res.*** **2005.** 46: **535–546.**

Supplementary key words differential scanning calorimetry • Langmuir monolayer • liposomes • lipid phase transition • head-tail mismatch

Nicotinic acid and its alkyl esters are of considerable biological and pharmacological importance. Besides being the precursor of cofactors to many vital enzymes, nicotinic acid is a drug possessing vasodilating and fibrinolytic properties. Nicotinic acid itself has been proven beneficial against bleomycin- and cyclophosphamide-induced lung injury in animal models (1–5). Dietary supplements of nicotinic acid and dermatologic formulations of its long-chain esters are under investigation for the prevention and treatment of skin carcinogenesis (6). Therefore, nicotinic acid esters may be useful as a chemopreventive agent for the prevention of lung cancer.

Currently, there is significant interest in the pulmonary administration of several chemopreventive agents, such as steroids and retinoids, directly to the lung because of reduced systemic toxicity (7–11). This route of administration may also be advantageous for the administration of nicotinic acid esters, by using either an aerosol or a perfluorocarbon vehicle (12, 13). Although the interaction of various chemopreventive agents, especially retinoids, with phospholipids has been investigated (14, 15), there is no current knowledge about the factors that determine the interaction (i.e., phase behavior) of nicotinates with biological lipids such as the phospholipids present in pulmonary surfactant. A better understanding of these interactions, however, is a prerequisite for the rational design of nicotinates for pulmonary administration, especially using a perfluorocarbon-based drug delivery system (12, 13). The aim of this study is to understand which molecular characteristics influence the phase behavior of phospholipid-nicotinate mixtures.

This study used a combination of monolayer and differential scanning calorimetry (DSC) studies to gain a better insight into the interaction of dipalmitoylphosphatidylcholine (DPPC), an important biological phospholipid, and several long-chain nicotinates. Monolayer studies using DPPC at the air-water interface were chosen as a model of the pulmonary surfactant. This method allows the direct investigation of lipid mixtures and their miscibility at the air-water interface. DSC, on the other hand, is a straightforward tool to investigate the effect of increasing incorporation of organic compounds (e.g., nicotinates) in organic bilayers (16). This technique allows the study of the effect of a compound dispersed in a (model) biological membrane on the gel-to-liquid or main transition

Manuscript received 14 October 2004 and in revised form 26 November 2004.

Published, JLR Papers in Press, December 16, 2004.
DOI 10.1194/jlr.M400406-JLR200

[1] To whom correspondence should be addressed.
e-mail: hans-joachim-lehmler@uiowa.edu

[S] The online version of this article (available at http://www.jlr.org) contains supplemental information.

characteristic for fully hydrated phospholipids when heated (17, 18). Changes in the onset of the so-called pretransition of phosphatidylcholines are another sensitive way to assess the interaction of an organic compound with a model lipid bilayer of this type of phospholipid. Overall, the combination of these two different approaches will further our understanding of phospholipid-nicotinate interactions and contribute to the rational design of nicotinates for pulmonary administration.

MATERIALS AND METHODS

The synthesis of the nicotinates followed literature procedures (13, 19). Their characterization and purity are described in detail in the supplemental information online. The analytical data for each compound are in good agreement with literature data (20). DPPC was obtained from Avanti Polar Lipids at >99% purity and used without further purification. 2-Propanol, chloroform, methanol and *n*-hexanes were HPLC grade and were purchased from Fisher Scientific or VWR. Concentrated hydrochloric acid was obtained from Fisher Scientific. Deionized water for the monolayer studies was distilled first from basic potassium permanganate followed by distillation from sulfuric acid (16, 19, 21–23). Deionized water for the DSC experiments was obtained from a Purelab Plus water system and had a resistance of ⩾18 Ω (16).

Monolayer experiments

All monolayer experiments were carried out in a rectangular Teflon trough (306 × 150 mm) held at 37 ± 2°C (KSV-3000; KSV Instruments Ltd., Helsinki, Finland). The surface pressure was measured by the Wilhelmy plate method using paper plates (15 × 58 mm) as described previously (16, 19, 21–24). Every surface area-surface pressure isotherm was determined on a freshly poured subphase (hydrochloric acid, pH 1.9–2.1). The subphase was allowed to equilibrate for 10 min at 37 ± 2°C. Surface-active impurities were removed from the air-water interface with a slight vacuum after compression of the barrier. Nicotinate, DPPC, and DPPC-nicotinate solutions with a concentration of 1–2 mg/ml were freshly prepared every day in *n*-hexane/2-propanol (9:1, v/v). A known quantity of solutions was spread on the surface, and 10 min at 37 ± 2°C was allowed to elapse for solvent evaporation before the start of the compression. A constant compression speed of 15 cm^2/min (10 mm/min) was used. Depending on the shape (i.e., collapse pressure) of the respective compression isotherm, the compression time was typically 15–20 min.

Preparation of samples for DSC

Calculated amounts of DPPC and nicotinate were dissolved in chloroform-methanol (3:1, v/v) at the appropriate mole fractions (25). The solvent was removed under a stream of nitrogen, and the mixtures were further dried under vacuum for at least 3 h. The samples (a mixture of phospholipid and nicotinate or pure phospholipid) were hydrated in an excess of water (three times by weight). Samples were heated above the lipid transition temperature for 5 min and vortexed for 2 min. This process was repeated four times. Finally, the samples were sonicated in a water bath above the lipid transition temperature for 30 min, followed by the heating and vortexing cycle mentioned above. Samples were stored at 4°C for 12–16 h. Hydration of samples was always carried out the day before collecting the DSC scans.

A Thermal Analysis 2920 differential scanning instrument was used for the DSC studies. The hydrated samples were weighed into DSC aluminum pans. The DSC cell and the refrigerated cooling system were purged with 60 and 120 ml/min dry nitrogen, respectively. Samples were cooled to 4°C at a cooling rate of 10°C/min and then heated from 4°C to 80°C with a heating rate of 5°C/min (16, 24–26). All samples were subjected to two subsequent heating cycles. All experiments were carried out in triplicate. Onset, maximum, and offset temperatures, as well as peak width of the pretransition and the main phase transition, were determined for the second run using Universal Analysis NT software (16, 19, 22, 24).

Calculation of molecular descriptors and packing parameter

Cross-sectional areas and other molecular descriptors of the nicotinates (e.g., tail length and molar volume) were calculated with Material Studio Modeling suite 3.0.1 (Accelrys, Inc., Cambridge, UK) after energy minimization using AM1 theory (27). The packing parameter of all four nicotinates was calculated as V/lA, where V is the volume of the entire surfactant molecule, l is its length, and A is the area of the nicotinate headgroup at the lipid-water interface (28).

RESULTS

The present study investigates the mixing behavior of four nicotinates with DPPC in insoluble monolayers at the air-water interface and in completely hydrated mixtures using DSC. The structures of the four nicotinates are shown in **Fig. 1**.

Behavior of long-chain nicotinates at the air-water interface

Lung fluid has been shown to have an acidic pH as low as pH 5.2 in certain types of lung disease. Therefore, we decided to investigate the behavior of the nicotinates on an acidic (i.e., hydrochloric acid) subphase at pH 1.9–2.1. Although this is more acidic compared with the typical physiological conditions in the lung, this subphase was chosen to allow a direct comparison with previous studies (16, 19, 21–24). Under the conditions of our study, all four long-chain nicotinates formed insoluble monolayers at the air-water interface (**Fig. 2**). None of the nicotinates appeared to form stable monolayers on unbuffered water (pH ∼ 7). The limiting molecular areas of the condensed phase of nicotinates are very similar and typically range from 24.6 to 28.6 $Å^2$/molecule over the entire temperature range studied (**Table 1**). The only exception is NA15, which forms an expanded phase at ⩾37 ± 2°C and, therefore, has a larger limiting molecular area of 44.9 $Å^2$/molecule at and above this temperature.

All compression experiments were performed at a pH of ∼1.9–2.1. The pyridine ring of the nicotinates is therefore completely protonated [the pyridine ring has a pk_a

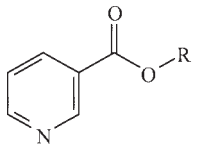

NA15: R = $-(CH_2)_{14}CH_3$
NA16: R = $-(CH_2)_{15}CH_3$
NA17: R = $-(CH_2)_{16}CH_3$
NA18: R = $-(CH_2)_{17}CH_3$

Fig. 1. Chemical structures of long-chain nicotinates.

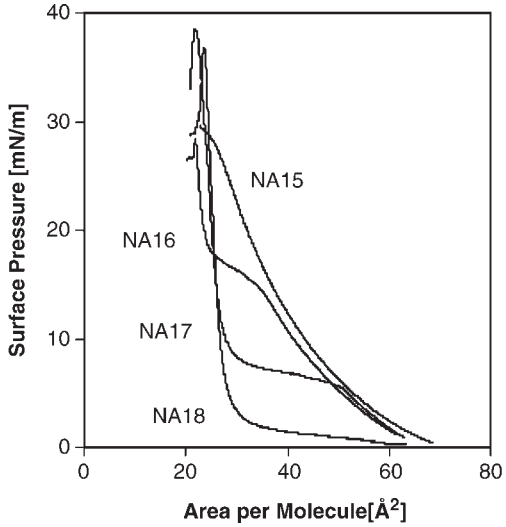

Fig. 2. Comparison of representative compression isotherms of the four nicotinates NA15, NA16, NA17, and NA18 at 37 ± 2°C on hydrochloric acid (pH 1.9–2.1).

value of 5.23 (29)]. As shown in Fig. 2, the compression isotherms of NA15 at physiological temperature (37 ± 2°C) show an expanded phase, whereas NA16 and NA17 exhibited a breakpoint characteristic of a phase transition from an expanded to a condensed state at this temperature. NA18 forms a condensed phase at this temperature. To verify that the breakpoints of NA16 and NA17 are attributable to a phase transition, the compression isotherms for each compound were recorded at different temperatures and the temperature dependence of the compressional onset of the phase transition was investigated. **Fig. 3A** shows the results for NA16. As summarized for all five nicotinates in Fig. 3B, the compressional onset of the phase transition of all five compounds is temperature dependent and can be observed over a fairly large temperature range of ~11.5°C (NA16) to 17°C (NA17). The temperature of the phase transitions depends of the length of the hydrocarbon chain, with longer molecules experiencing the transitions at higher temperatures. **Figure 4** shows the chain length dependence of T_0, the lowest temperature at which an expanded state can exist (30). For comparison, the melting points (T_M) of the nicotinates are shown as well. T_0 was estimated by linear regression of the data points in Fig. 3B. Although the number of compounds under investigation is limited, there appears to be no odd-even chain length effect on T_0. In contrast, an odd-even chain length effect was observed for the T_M of the four nicotinates.

TABLE 1. Temperature dependence of the limiting molecular area, collapse pressure, and phase transition of nicotinates NA15 through NA18 on hydrochloric acid (pH 1.9–2.1)

Temperature	Limiting Molecular Area	Collapse Pressure	Phase Transition
	Å²/molecule	*mN*	*mN/m*
NA15			
37.0	44.9 ± 1.6	30.1 ± 0.6	None
31.5	28.2 ± 0.7	34.8 ± 0.6	20.4 ± 0.5
25.5	27.1 ± 2.1	35.8 (n = 2)	12.1 ± 0.3
19.5	26.0 ± 0.7	39.1 ± 0.5	6.9 ± 0.2
17.0	26.3 ± 0.9	43.4 ± 0.8	5.2 ± 0.3
14.5	24.6 ± 1.0	46.3 ± 0.6	3.4 ± 0.3
NA16			
50.0	46.8 ± 2.4	27.7 ± 0.2	None
37.0	27.0 ± 0.8	28.8 ± 0.5	15.0 ± 0.1
32.5	26.6 ± 0.3	33.6 ± 0.8	9.8 ± 0.3
30.0	26.2 ± 0.7	30.9 ± 1.8	7.1 ± 0.3
27.5	26.5 ± 0.4	34.7 ± 0.6	5.4 ± 0.1
25.5	26.2 ± 1.0	33.4 ± 0.8	4.0 ± 0.2
19.5	25.4 (n = 1)	35.8 (n = 1)	None
NA17			
44.0	29.2 ± 0.2	>30.5	12.3 ± 0.4
40.0	28.0 ± 0.2	37.2 ± 1.2	8.4 ± 0.3
37.0	28.6 ± 0.4	37.9 ± 0.6	5.5 ± 0.1
30.0	26.2 ± 0.4	47.3 ± 0.8	1.3 ± 0.1
21.0	25.7 ± 0.1	54.8 ± 1.7	None
NA18			
44.0	32.4 ± 2.9	25.4 ± 0.8	5.7 ± 0.5
40.0	26.6 ± 0.6	32.6 ± 0.6	2.3 ± 0.1
37.0	27.2 ± 1.0	37.4 ± 1.9	None
30.0	26.0 ± 0.3	46.0 ± 0.5	None

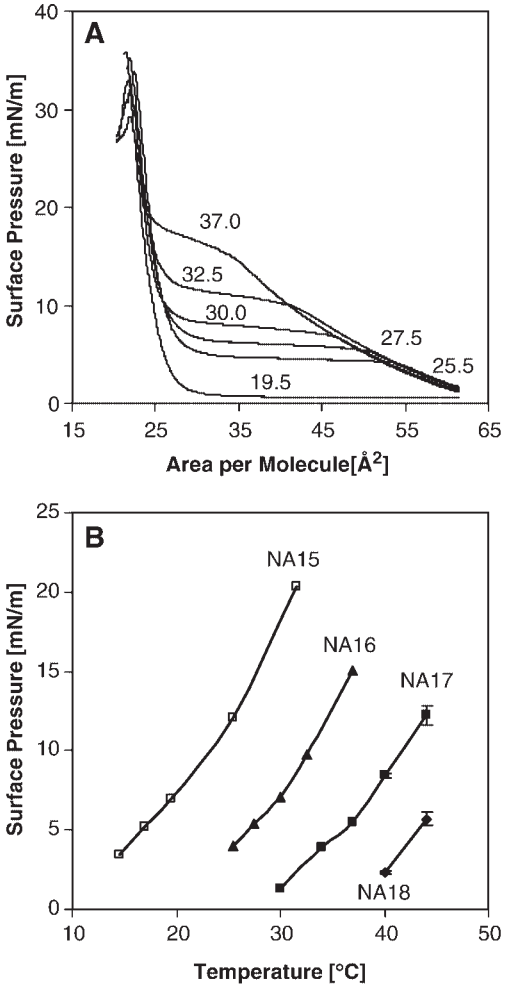

Fig. 3. Temperature dependence of the compression isotherms of long-chain nicotinates on hydrochloric acid (pH 1.9–2.1). A: Compression isotherms of NA16. B: Temperature dependence of the breakpoint of the phase transition of the four nicotinates. All data points are averages of at least three experiments ± SD.

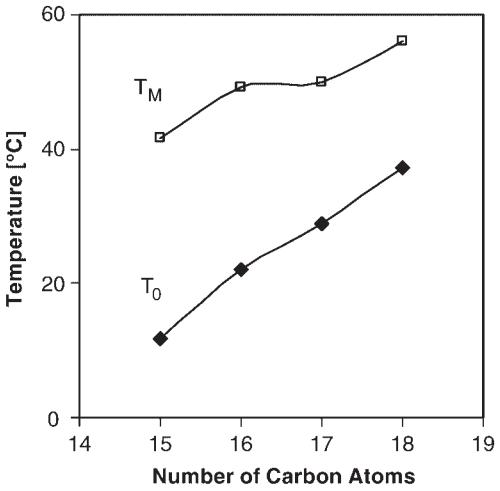

Fig. 4. Chain length dependence of T_0 (the lowest temperature at which an expanded state can exist) and the melting temperature (T_M; maximum of phase transition) for the homologous series of nicotinates NA15 to NA18. Closed diamonds, T_0; open squares, T_M.

Interaction of nicotinates with DPPC at the air-water interface

The concentration dependence of the breakpoint(s) of the phase transition of the compression isotherms was used as a criterion for the miscibility of binary mixtures at the air-water interface (16, 21, 23, 31, 32). In short, a concentration-dependent phase transition is indicative of complete miscibility of the components, whereas concentration independence is a sign of immiscibility of the components (31). Because of experimental limitations, the collapse pressure of the compression isotherms of most mixtures was not recorded and, therefore, was not used to assess the miscibility of the mixed films.

The concentration dependence of the average molecular area at constant film pressure is a second criterion used to assess the miscibility of two components at the air-water interface. In ideal behavior, the average area per molecule of any mixture is the sum of the areas occupied by each species at the surface:

$$A(\pi) = X_{Nicotinate} \times A_{Nicotinate} + X_{DPPC} \times A_{DPPC} \quad (Eq.\ 1)$$

where X is the mole fraction of each component present at the air-water interface, A is the average area per molecule of the pure component, Nicotinate is the respective nicotinate, and DPPC is dipalmitoylphosphatidylcholine. This equation is often referred to as the "additivity rule." Mixtures of two components that follow equation 1 show either ideal mixing or complete phase separation. Binary mixtures that do not follow equation 1 exhibit (partial) miscibility resulting from interactions between the two components. An attractive interaction will lead to a negative deviation from ideal behavior, and a repulsive interaction will lead to a positive deviation. To investigate their mixing behavior, the compression isotherms of mixtures of the respective nicotinate and DPPC were recorded at various compositions at 37 ± 2°C (**Fig. 5**). The breakpoints of the phase transitions for all $\pi - A$ isotherms were determined where applicable and are summarized in **Fig. 6**. The $A - X_{DPPC}$ diagrams (equation 1) of all carboxylic acid-phosphatidyl choline mixtures are shown at several surface pressures in **Fig. 7**.

DPPC and NA15

As shown in Fig. 5A, with the exception of pure NA15, a phase transition from an expanded to a condensed phase can be observed for all compression isotherms of this mixture. As shown in Fig. 6A, the surface pressure at which this phase transition occurs increases with increasing mole fraction of NA15. This phase-dependent change in the compressional onset of the phase transition suggests at least partial miscibility of the two components. This assessment is supported by a negative deviation from equation 1 for all surface pressures analyzed (Fig. 7A).

DPPC and NA16

In this mixture, a transition from an expanded to a condensed phase can be observed for all compression isotherms (Figs. 5B, 6B). The surface pressure of the onset of the phase transition appears to be independent of the concentration for all four DPPC-NA16 mixtures investigated (Fig. 6B); however, there is a change in the onset of the phase transition between X_{DPPC} = 0–0.2 and X_{DPPC} = 0.8–1. The A − X diagram in Fig. 7B shows a very slight negative deviation from equation 1 at low surface pressures of 3 and 7 mN/m. A different behavior can be observed at a surface pressure of 20 mN/m. At low mole fractions of DPPC (X_{DPPC} = 0–0.6), a positive deviation from equation 1 can be observed, whereas in the high mole fraction range above $X_{DPPC} > 0.6$, ideal behavior can be observed. These characteristics in the A − X diagram are the result of the phase transition that occurs at this surface pressure range (for a detailed discussion of how phase transitions appear in A − X diagrams, see 33). Overall, the phase behavior suggests that this mixture is partially miscible but to a lesser extent compared with the DPPC-NA15 system.

DPPC and NA17

The compression isotherms of the pure compounds as well as the four mixtures investigated show a concentration-dependent compressional onset of a phase transition from an expanded to a condensed phase (Figs. 5C, 6C). The surface pressure of the onset increases with decreasing content of nicotinate NA17 until a maximum is reached at approximately $X_{DPPC} \sim 0.7$ and decreases slightly thereafter. The phase transition occurs in a fairly large surface pressure range between 5 and 25 mN/m, thus resulting in a complex A − X diagram (Fig. 7C) with both positive and negative deviations from equation 1 at 7 and 20 mN/m, respectively. However, at 3 mN/m, a clear but small negative deviation from equation 1 can be observed. Based on these two observations, the DPPC-NA17 system shows evidence of partial miscibility.

DPPC and NA18

The compression isotherm of pure NA18 is of the condensed type and exhibits no phase transition at physiolog-

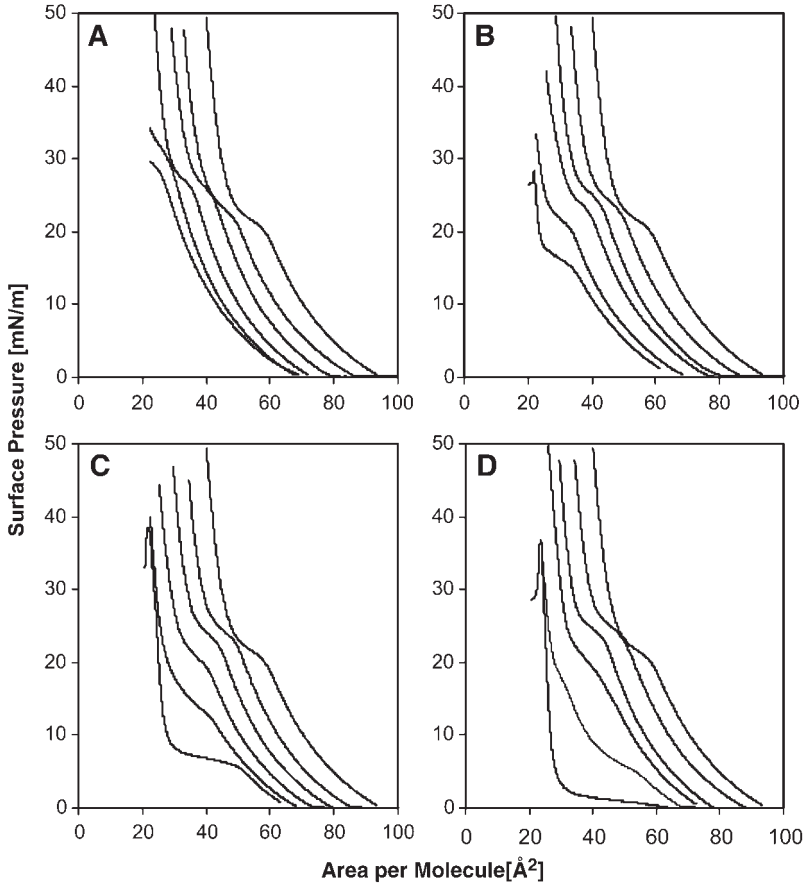

Fig. 5. Compression isotherms of mixtures of dipalmitoylphosphatidylcholine (DPPC) with NA15 (0, 0.20, 0.39, 0.60, 0.79, 1) (A), NA16 (0, 0.20, 0.41, 0.60, 0.80, 1) (B), NA17 (0, 0.20, 0.39, 0.60, 0.78, 1) (C), and NA18 (0, 0.20, 0.40, 0.60, 0.80, 1) (D) at 37 ± 2°C on hydrochloric acid (pH 1.9–2.1). Numbers in parentheses are the mole fractions of DPPC (from left to right).

ical temperature, whereas the compression isotherms of all four DPPC-NA18 mixtures as well as pure DPPC exhibit a phase transition from an expanded to a condensed phase (Fig. 5D). Interestingly, the compression isotherm at a mole fraction of $X_{DPPC} = 0.2$ appears to exhibit two distinct phase transitions. There appears to be a constant phase transition at low mole fractions of DPPC [i.e., $X_{DPPC} \leq 0.4$ (Fig. 6D)]. Above a mole fraction of DPPC = 0.4, the surface pressure of the onset of the phase transition increases with a maximum between $X_{DPPC} = 0.7$–0.8 and shows a decrease thereafter. The data presented in Fig. 6D suggest that the DPPC-NA18 mixture is partially miscible. The A − X diagram shown in Fig. 7D is very complex because of the phase transition(s), thus making it difficult to support these conclusions regarding the miscibility of DPPC and NA18.

Interactions of DPPC and long-chain nicotinates in an excess of water studied by DSC

The thermograms of mixtures of the four nicotinates NA15, NA16, NA17, and NA18 are shown in **Fig. 8**. At mole fractions of DPPC < 0.7, several of the DPPC-nicotinate mixtures show a complex phase behavior, indicating the presence of several lipid assemblies, some rich and some poor in nicotinate. This makes an interpretation of the phase diagrams at higher nicotinate concentrations difficult; therefore, we decided against analyzing the biologically less relevant part of the phase diagrams with high nicotinate concentrations (i.e., $X_{DPPC} < 0.5$).

DPPC and NA15

The DSC scans of DPPC-NA15 dispersions are shown in Fig. 8A and a partial phase diagram is shown in **Fig. 9A**. In addition to the main transition, an early transition can be observed over the entire concentration range studied. Down to a concentration of $X_{DPPC} \sim 0.8$, this peak resembles the pretransition of pure DPPC. As shown in Fig. 9A, the onset temperature of this putative pretransition increases with increasing concentration of the nicotinate and reaches a plateau at a mole fraction of DPPC ~ 0.8. At a mole fraction of DPPC = 0.7, a broad, shoulder-like, early transition can be observed. At mole fractions of DPPC = 0.5, two distinct phase transitions can be observed, with the earlier transition being less intense.

This main (or second) phase transition occurs between 39°C to 44°C over the concentration range under investigation. For comparison, the onset of the T_M of the pure nicotinate is 39°C and decreases exactly in the range of

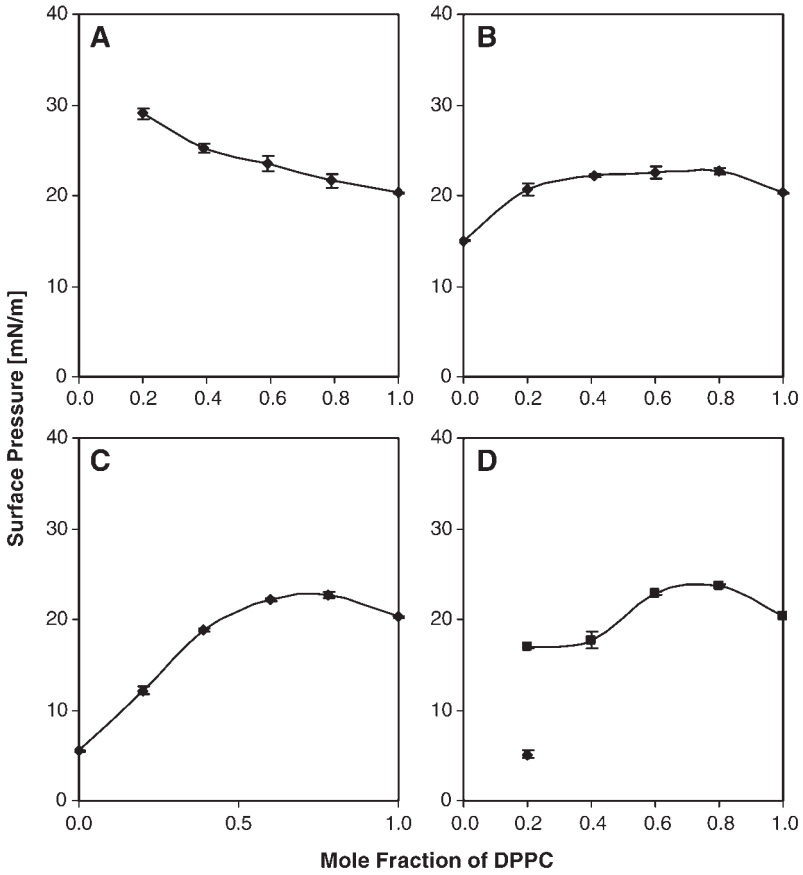

Fig. 6. Mole fraction dependence of the phase transition of mixtures of DPPC with NA15 (A), NA16 (B), NA17 (C), and NA18 (D) at 37 ± 2°C on hydrochloric acid (pH 1.9–2.1). All data points are averages of at least three experiments ± SD.

this phase transition. This main phase transition shows a slight decrease in the onset temperature and remains constant at $X_{DPPC} \geq 0.8$. Within the experimental error, the half-width of this transition does not show a significant change above a mole fraction of DPPC = 0.8. Because two peaks are present at mole fractions of $X_{DPPC} \geq 0.8$, the phase transitions occur over a larger temperature range, resulting in a large half-width of the combined peaks.

DPPC and NA16

The thermograms of this mixture are shown in Fig. 8B. A partial phase diagram is shown in Fig. 9B, with the dotted line representing the onset of the T_M of pure NA16. Similar to the DPPC-NA15 mixture, increasing amounts of NA16 result in a slight decrease of the onset temperature of the main phase transition. Down to a mole fraction of DPPC = 0.91, a pretransition can be observed that is distinctly separate from the main phase transition. This pretransition shows a very slight decrease in its onset with increasing mole fraction of the nicotinate. At $X_{DPPC} \leq 0.81$, the main phase transition broadens and a shoulder can be observed at lower temperatures. This may be attributable, in part, to the pretransition merging with the main transition peak; however, as is evident in the DSC curves at mole fractions of DPPC = 0.7 and 0.5, additional phase transitions seem to appear in this concentration range. This results in a broad temperature range over which the lipid assemblies melt; however, the onset temperature of this transition range is fairly constant, as shown in Fig. 9B. There is no evidence of a transition at 39°C, as would be expected of the formation of a nicotinate-rich phase.

DPPC and NA17

The DSC curves and partial phase diagram of this mixture are shown in Figs. 8C, 9C, respectively. The pretransition of DPPC decreases with the increasing mole fraction of NA17 and shows a significant peak broadening. The pretransition is abolished at a mole fraction of DPPC < 0.91. The main phase transition shifts to lower temperatures and shows some peak broadening in the mole fraction range between X_{DPPC} = 1–0.85. At a mole fraction of DPPC < 0.85, the peak of the main phase transition broadens significantly (i.e., exhibits a shoulder at lower temperatures) while the onset temperature of this transition remains constant. As shown in Fig. 8C, a second phase transition representative of a higher T_M, nicotinate-rich lipid assembly occurs at higher temperatures below a mole fraction of DPPC = 0.85. For comparison, the onset of the T_M of NA17 is shown in Fig. 9C as a dotted line.

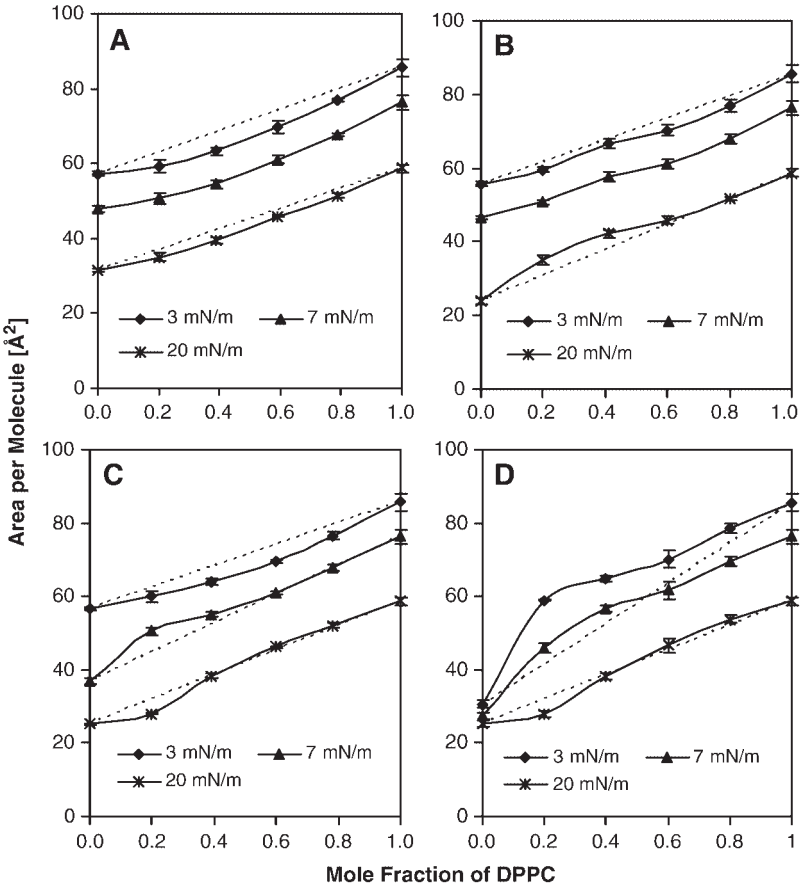

Fig. 7. A − X_{DPPC} diagrams of mixtures of DPPC with NA15 (A), NA16 (B), NA17 (C), and NA18 (D) at 37 ± 2°C on hydrochloric acid (pH 1.9–2.1). All data points are averages of at least three experiments ± SD.

DPPC and NA18

Figures 8D, 9D show the thermograms and a partial phase diagram of this mixture, respectively. The onset of the pretransition of DPPC occurs at decreasing temperatures with increasing concentrations of NA18. The peak of the pretransition broadens significantly and merges with the main transition by forming a shoulder at mole fractions of DPPC < 0.98. The pretransition is abolished below a mole fraction of DPPC = 0.91. Up to $X_{DPPC} > 0.77$, the onset of the main phase transition decreases with increasing nicotinate concentration. In this concentration range, the main phase transition also shows some peak broadening. Starting at a mole fraction of DPPC = 0.77, a broad main phase transition can be observed. The peak shape of the transition (i.e., the presence of two maxima at X_{DPPC} = 0.66 and 0.6) suggests the presence of several lipid assemblies, including the one present at higher DPPC mole fractions (see T_M of the main phase transition in Fig. 9D). The onset of this transition remains constant between X_{DPPC} = 0.77 and 0.6. As shown in Figs. 8D, 9D, at mole fractions of DPPC ≤ 0.66, several additional phase transitions can be observed at higher temperatures. These additional phase transitions occur slightly below the T_M of pure NA18 (dotted line in Fig. 9D), suggesting the presence of NA18-rich lipid phases.

DISCUSSION

Unfortunately, hydrochloric acid, which was used as subphase in the monolayer studies, cannot be used with DSC pans made from alumina. Thus, the differences in pH should be taken into consideration when comparing the monolayer and DSC studies. Under the acidic conditions (pH 1.9–2.1) used for the monolayer studies, the phosphate residue of DPPC (34) and the pyridine moiety of the nicotinates are expected to be protonated. This is not the case for the DSC studies, which were performed at pH 7. Thus, the structures and charge distribution of the phosphatidylcholine and the nicotinate headgroups as well as their immediate water shells are expected to differ significantly between the monolayer and DSC experiments. Despite the resulting structural differences of the monolayers and bilayers, these two studies still provide an insight into packing constraints in the DPPC-nicotinate assemblies and answer the question of whether nicotinates can partition into DPPC monolayers and bilayers.

Monolayer studies of pure nicotinates

In contrast to short-chain nicotinates (<8 carbon atoms) (13), long-chain nicotinates (>14 carbon atoms) have a limited solubility in water (20). Therefore, it was

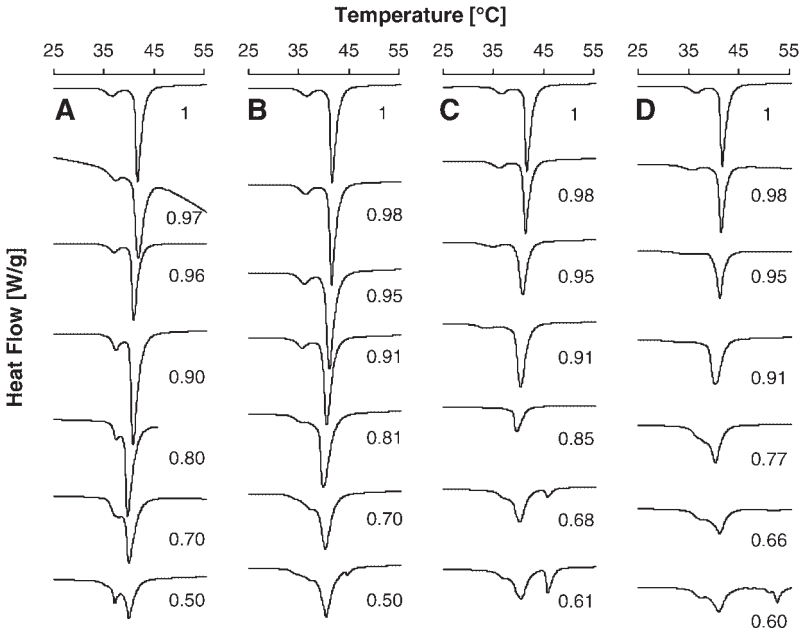

Fig. 8. Typical calorimetric scans for mixtures of DPPC with NA15 (A), NA16 (B), NA17 (C), and NA18 (D) in excess water. The mole fraction of DPPC is indicated beside each scan. The heating rate was 5°C/min from 4°C to 80°C (only the part of the curve with a phase transition is shown).

expected that the long-chain nicotinates would form insoluble monolayers at the air-water interface. Indeed, all four nicotinates formed insoluble monolayers on a hydrochloric acid subphase over a wide temperature range (Table 1). Depending on the temperature of the subphase, the limiting molecular area of the nicotinates was between 24 and 29 Å^2. Overall, these values are significantly larger than the limiting molecular area of 20 Å^2/molecule of

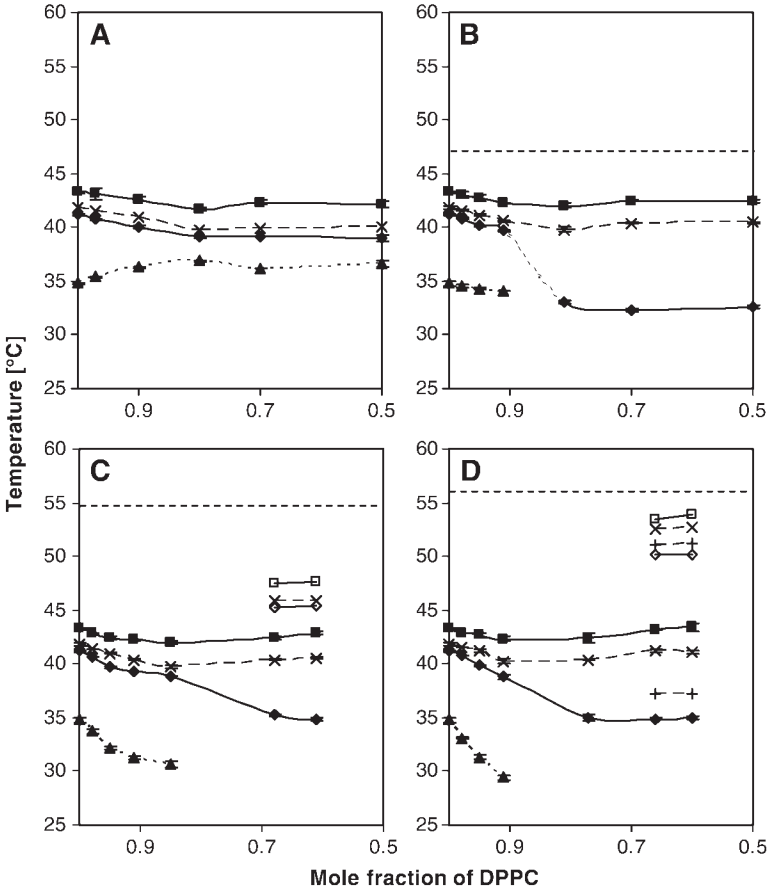

Fig. 9. Partial phase diagram of mixtures of DPPC with NA15 (A), NA16 (B), NA17 (C), and NA18 (D) in excess water. Closed triangles, onset temperature of the pretransition; closed and open diamonds, onset temperature of a main transition; closed and open squares, offset temperature of a main transition. × and + represent maxima within a phase transition. The dotted line represents the T_M of the pure long-chain nicotinate. The T_M of NA15 is not shown because its T_M and the major phase transition of DPPC are almost identical (A). All data points are averages of at least three experiments ± SD.

typical long-chain hydrocarbon carboxylic acids or alcohols (35). The larger limiting molecular area likely reflects a larger headgroup size. The areas of the protonated and unprotonated nicotinates were calculated to be 24.3 and 25.2 Å^2, respectively. To verify that these results represent realistic estimations of the limiting molecular area of a surfactant at the air-water interface, we also calculated the limiting molecular area of DPPC. The calculated limiting molecular area of DPPC = 48.8 Å^2 is in good agreement with the experimental headgroup size of 46 Å^2 (21, 36, 37). The limiting molecular area of the nicotinates, therefore, reflects the size of the protonated nicotinic acid headgroup at the air-water interface. Based on these results, the nicotinates show a head-tail mismatch, with the headgroup being larger compared with the hydrophobic hydrocarbon tail. This head-tail mismatch is expected to affect the packing of the hydrocarbon tails and, ultimately, the stability of the respective monolayers.

A shown in Fig. 3B and Table 1, the compression isotherms of all four nicotinates have a temperature-dependent transition from an expanded to a condensed phase. This phase transition occurs over a relatively large temperature range of ~12–17°C for the nicotinates NA15 to NA17 as well as a large surface pressure range of ~11–17 mN/m. At lower temperatures, the transition region of the nicotinate is relatively large as well (i.e., the surface pressure at lower temperatures remains almost constant) (Fig. 3A), suggesting a first order phase transition. Higher order transitions can be observed toward the putative triple point of the phase diagram (i.e., with increasing temperatures). On a side note, the extended transition region was the reason why we were unable to determine the collapse pressure for most compression isotherms. With our experimental setup, it was impossible to begin the compression of most mixtures at or near zero surface pressure and compress the monolayer to its collapse.

Within this series, the temperature of the phase transition depends on the length of the hydrocarbon chain, with longer nicotinates experiencing the phase transition at higher temperatures (Fig. 3B). A variety of amphiphiles, such as carboxylic acids (38, 39) and phospholipids (40, 41), show a similar chain length dependence for the onset of an expanded-condensed phase transition (for review, see 42). For example, for simple carboxylic acids, the phase transition is systematically shifted along the temperature axis by 5–10°C per additional methylene group (39). A similar observation can be made for the homologous series of the nicotinates.

Odd-even alterations of physical properties such as the T_M are characteristic for most bulk compounds, including carboxylic acids and phospholipids, but they have also been investigated for some compounds at the air-water interface (40, 41). Within this series of nicotinates, T_0, the lowest temperature at which an expanded state can exist (30), was estimated using linear regression. T_0 exhibited no apparent odd-even effect, whereas such an effect, although not very pronounced, was observed for the T_M of the nicotinates.

Monolayer studies of DPPC-nicotinate mixtures

To the best of our knowledge, the mixing behavior of nicotinates (or nicotinic acid) with phospholipids has not been investigated previously at the air-water interface. The mixtures of the nicotinates NA15 to NA18 appear to be partially miscible at the air-water interface (hydrochloric acid at 37 ± 2°C). This interpretation of our monolayer studies is supported by the presence of concentration-dependent breakpoints of a phase transition from a liquid-expanded to a liquid-condensed phase. Such a phase transition is present in all four mixtures over practically the entire concentration range. The mixtures of DPPC with NA16 and NA17 have maxima in the phase diagram shown in Fig. 6B, C. A number of binary mixtures containing tetradecanoic or pentadecanoic acid and an ester of an acid or alcohol with similar chain length are known to exhibit similar behavior at the air-water interface (43). Matuo, Motomura, and Matuura (43) refer to these systems as the "positive azeotropic type" because of the maximum point in the phase diagram. At this maximum, the two-dimensional azeotropic point, the mole fractions of the expanded and condensed phases are equal. The components of these systems are miscible in both phases. It is notable that mixtures of the positive azeotropic type have components with a bulky headgroup.

The interpretation of the DPPC-nicotinate systems as partially miscible is in several cases supported by a negative deviation from equation 1 in the A − X diagrams. Unfortunately, the A − X diagrams are less helpful in accessing the miscibility in the DPPC-nicotinate mixtures because of the phase transition(s) that can be observed over wide concentration and surface pressure ranges, thus making an unambiguous interpretation of the A − X diagrams difficult. For the same reason, an unambiguous assessment of a trend in the (partial) miscibility in this homologous series of surfactants using the extent of the negative deviation from equation 1 is difficult. It appears that increasing the chain length of the nicotinate results in less miscibility with DPPC. The appearance of two distinct phase transitions at low mole fractions of DPPC in the DPPC-NA18 system (i.e., a deviation from the inverse U-shaped phase diagram of the shorter analogs) is probably the best evidence for decreasing miscibility with increasing chain length.

DSC studies of fully hydrated nicotinate-DPPC mixtures

As can be seen in Fig. 8, the thermal properties of the DPPC-nicotinate mixtures are very complex. With a decreasing mole fraction of the phospholipids, several phase transitions can be observed, which indicates the presence of several different lipid assemblies. Most notable is the occurrence of higher-melting-point assemblies at higher concentrations of the nicotinate for NA17 and NA18 (i.e., $X_{DPPC} < 0.7$). These transitions occur at temperatures between the main gel-to-liquid phase transition of DPPC and the T_M of the respective nicotinate (Figs. 8, 9), suggesting that these lipid assemblies are nicotinate-rich. In contrast to these two longer chain nicotinates, NA16 shows no such higher melting point, possibly nicotinate-rich phases

down to a mole fraction of DPPC = 0.5. Because the main phase transition of DPPC and the T_M of NA15 overlap, it is not possible to determine from the DSC data whether similar phases exist in this system. Overall, these data suggest that the four nicotinates are associated or miscible with the phospholipid at low mole fractions of DPPC (i.e., $X_{DPPC} < 0.5$ for NA16 and possibly NA15 as well as $X_{DPPC} < 0.7$ for NA17 and NA18). The occurrence of nicotinate-rich phases at mole fractions of DPPC < 0.7 for NA17 and NA18 suggests that the miscibility of the nicotinates with DPPC decreases with increasing chain length of the nicotinate. These findings are in agreement with our monolayer studies, which also suggest a decrease of miscibility with increasing chain length in the composed film at the air-water interface.

Our data clearly suggest that the lipid is associated with DPPC, probably with the unprotonated nicotinic acid headgroup located at the water-lipid interface. Assuming such an orientation of the nicotinates, the complex phase behavior of DPPC-nicotinate mixtures can be interpreted on the basis of the geometric packing properties of the two different surfactants (i.e., their respective packing parameters) (44). DPPC with a packing parameter between 0.5 and 1 favors the formation of bilayers. We estimated a packing parameter of 0.52 using the definition by Marsh (28) and a parameter of 0.76 using the formulas given by Israelachvili (44) for all four nicotinates. This packing parameter suggests that the nicotinates, like DPPC, favor the formation of curved, flexible bilayers (44). Assuming additivity of the packing parameters, mixtures of nicotinates and DPPC are likely to form a variety of lipid assemblies with a curved bilayer structure and an asymmetric distribution of DPPC and the nicotinate in the bilayer (45). Another possible explanation for the complex phase behavior is the formation of mixed micelles. Like many other single-tail surfactants, nicotinates may be expected to form mixed micelles, but the packing parameter does not support the formation of such structures; however, the formation of other lipid assemblies cannot be excluded.

The pretransition of DPPC (18) exhibits a complex behavior in the presence of increasing mole fractions of the nicotinates. Frequently, the addition of small molecules to DPPC reduces or eliminates the pretransition at low concentrations (46). For example, under the same conditions used in this study, mixtures of perfluorinated and partially fluorinated acids with phosphatidylcholines result in the elimination of the pretransition (16, 24). In these mixtures, a more optimal (i.e., vertical) alignment of the tails is possible in the presence of small quantities of carboxylic acids and other small molecules, thus resulting in the elimination of the tilted gel phase and, hence, the pretransition. All four DPPC-nicotinate mixtures exhibit drastically different behavior with respect to this pretransition. In the DPPC-NA15 mixture, the onset of the pretransition increases until a maximum at $X_{DPPC} = 0.8$; however, at even lower mole fractions, the main transition seems to split into two transitions. Although this second transition occurs in the same temperature range as the pretransition, its peak shape is different from a typical pretransition peak, which makes it difficult to determine at which mole fraction the pretransition is eliminated. A similar behavior of the pretransition can be observed for the DPPC-NA16 mixture. The other two nicotinate mixtures show similar additional pretransition-like phase transitions below the original gel-to-liquid phase transition of DPPC; however, for both mixtures, the onset of the pretransition decreases with increasing concentration of NA17 or NA18 and is eliminated at $X_{DPPC} < 0.91$ or 0.95, respectively (Fig. 9).

These observations suggest that, unlike many other small molecules, the addition of small amounts of long-chain nicotinates to fully hydrated DPPC does not result in a more optimal vertical packing of the tails in the mixed bilayers. This observation can be easily explained by the fact that both DPPC and nicotinate have a larger headgroup compared with the hydrophobic tail. The nicotinates, therefore, cannot compensate for the head-tail mismatch of DPPC, and the hydrophobic tails need to adopt a tilted orientation in DPPC-nicotinate mixtures at any given mole fraction. The head-tail mismatch of both surfactants could explain the low-melting-point lipid assemblies (i.e., pretransition-like peaks) observed for all four DPPC-nicotinate mixtures. These may be phases with an increased tilt angle that accommodate the head-tail mismatch of both surfactants. With increasing concentration of the nicotinate, even a significant tilt angle cannot compensate for the combined head-tail mismatches, thus resulting in the formation of nicotinate-rich phases, as seen for the longer chain nicotinates NA17 and NA18.

In summary, all four long-chain nicotinates are surface active and form stable monolayers at the air-water interface. They are to some degree miscible with DPPC in monolayers at the air-water interface as well as fully hydrated DPPC. The miscibility decreases with increasing chain length within the series of nicotinates. These observations are thought to result from the head-tail mismatch of the respective nicotinate. Overall, our experimental findings suggest that in both the monolayer and the fully hydrated DPPC, the nicotinates are oriented parallel to DPPC. Although the phase behavior of the DPPC-nicotinate mixture can be interpreted on the basis of geometrical considerations such as the packing parameter, further studies are needed to fully characterize and understand the phase behavior and the underlying packaging constraints of these mixtures.

Our findings have implications for a variety of biomedical applications, such as pulmonary or transdermal drug delivery of these compounds as well as the biological effects of long-chain nicotinates. After pulmonary administration, these putative chemopreventive agents will first come in contact with the pulmonary surfactant and, subsequently, the cell membrane of pulmonary epithelial cells. To achieve therapeutically relevant lung tissue concentrations, the nicotinates need to partition through both the monolayer of the pulmonary surfactant and the bilayer of the epithelial cells. Our studies indicate that the

highly lipophilic long-chain nicotinates can, indeed, partition into lipid monolayers and bilayers, suggesting that especially the shorter chain derivatives (i.e., NA15) can partition into lung tissue. Our studies also indicate that the longer chain nicotinates are less miscible with DPPC. As a result, more complex lipid assemblies are formed in the presence of small amounts of these nicotinates (e.g., NA17 and NA18). This may ultimately result in an inhibition of pulmonary surfactant and alter bilayer function in endothelial cells. Nicotinates with a medium chain length of ~15 carbon atoms, therefore, may be more suitable for pulmonary administration. These findings may also apply to the transdermal delivery of long-chain nicotinates for the prevention of skin cancer.

This work was supported in part by a grant from the American Lung Association (RG-024-N) and a grant from the National Institute of Biomedical Imaging and Bioengineering (EB 02748). A.F-S. was supported by National Institute of Environmental Health Sciences (ES 10951).

REFERENCES

1. Gurujeyalakshmi, G., Y. Wang, and S. N. Giri. 2000. Suppression of bleomycin-induced nitric oxide production in mice by taurine and niacin. *Nitric Oxide.* **4:** 399–411.
2. Gurujeyalakshmi, G., Y. Wang, and S. N. Giri. 2000. Taurine and niacin block lung injury and fibrosis by down-regulating bleomycin-induced activation of transcription nuclear factor-kappaB in mice. *J. Pharmacol. Exp. Ther.* **293:** 82–90.
3. Giri, S. N., R. Blaisdell, R. B. Rucker, Q. Wang, and D. M. Hyde. 1994. Amelioration of bleomycin-induced lung fibrosis in hamsters by dietary supplementation with taurine and niacin: biochemical mechanisms. *Environ. Health Perspect.* **102:** 137–147.
4. Venkatesan, N., and G. Chandrakasan. 1994. In vivo administration of taurine and niacin modulate cyclophosphamide-induced lung injury. *Eur. J. Pharmacol.* **292:** 75–80.
5. Nagai, A., H. Matsumiya, M. Hayashi, S. Yasui, H. Okamoto, and K. Konno. 1994. Effects of nicotinamide and niacin on bleomycin-induced acute injury and subsequent fibrosis in hamster lungs. *Exp. Lung Res.* **20:** 263–281.
6. Jacobson, E. L., W. M. Shieh, and A. C. Huang. 1999. Mapping the role of NAD metabolism in prevention and treatment of carcinogenesis. *Mol. Cell. Biochem.* **193:** 69–74.
7. Wattenberg, L. W., and R. D. Estensen. 1997. Studies of chemopreventive effects of budesonide on benzo[*a*]pyrene-induced neoplasia of the lung and forestomach of female A/J mice. *Carcinogenesis.* **18:** 2015–2017.
8. Wattenberg, L. W., T. S. Wiedmann, R. D. Estensen, C. L. Zimmerman, A. R. Galbraith, V. E. Steele, and G. J. Kelloff. 2000. Chemoprevention of pulmonary carcinogenesis by brief exposures to aerosolized budesonide or beclomethasone dipropionate and by the combination of aerosolized budesonide and dietary *myo*-inositol. *Carcinogenesis.* **21:** 179–182.
9. Wang, D. L., M. Marko, A. R. Dahl, K. S. Engelke, M. E. Placke, A. R. Imondi, J. L. Mulshine, and L. M. De Luca. 2000. Topical delivery of 13-cis-retinoic acid by inhalation up-regulates expression of rodent lung but not liver retinoic acid receptors. *Clin. Cancer Res.* **6:** 3636–3645.
10. Dahl, A. R., I. M. Grossi, D. P. Houchens, L. J. Scovell, M. E. Placke, A. R. Imondi, G. D. Stoner, L. M. De Luca, D. Wang, and J. L. Mulshine. 2000. Inhaled isotretinoin (13-cis-retinoic acid) is an effective lung cancer chemopreventive agent in A/J mice at low doses: a pilot study. *Clin. Cancer Res.* **6:** 3015–3024.
11. Kohlhaufl, M., K. Haussinger, F. Stanzel, A. Markus, J. Tritschler, A. Muhlhofer, A. Morresi-Hauf, I. Golly, G. Scheuch, B. H. Jany, and H. K. Biesalski. 2002. Inhalation of aerosolized vitamin A: reversibility of metaplasia and dysplasia of human respiratory epithelia. A prospective pilot study. *Eur. J. Med. Res.* **7:** 72–78.
12. Lehmler, H-J., P. M. Bummer, and M. Jay. 1999. Liquid ventilation—a new way to deliver drugs to diseased lungs? *Chemtech.* **29:** 7–12.
13. Hsu, C-H., M. Jay, P. M. Bummer, and H-J. Lehmler. 2003. Chemical stability of esters of nicotinic acid intended for pulmonary administration by liquid ventilation. *Pharm. Res.* **20:** 918–925.
14. Itho, N., H. Komatsu, T. Handa, and K. Miyajima. 1995. Emulsion and vesicle formation of retinol and retinyl palmitate with egg yolk phosphatidylcholine. *J. Colloid Interface Sci.* **174:** 148–155.
15. Wiedmann, T. S., R. Bhatia, and L. W. Wattenberg. 2000. Drug solubilization in lung surfactant. *J. Controlled Release.* **65:** 43–47.
16. Arora, M., P. M. Bummer, and H-J. Lehmler. 2003. Interaction of a partially fluorinated heptadecanoic acid with diacyl phosphatidylcholines of varying chain length. *Langmuir.* **19:** 8843–8851.
17. Silvius, J. R. 1991. Thermotropic properties of phospholipid analogues. *Chem. Phys. Lipids.* **57:** 241–252.
18. Huang, C-h., and S. Li. 1999. Calorimetric and molecular mechanics studies of the thermotropic phase behavior of membrane phospholipids. *Biochim. Biophys. Acta.* **1422:** 273–307.
19. Lehmler, H-J., and P. M. Bummer. 2002. Behavior of 10-(perfluorohexyl)-decanol, a partially fluorinated analog of hexadecanol, at the air-water interface. *J. Fluorine Chem.* **117:** 17–22.
20. Badgett, C. O., R. C. Provost, C. L. Ogg, and C. F. Woodward. 1945. Nicotinic acid. Water-insoluble esters and amides. *J. Am. Chem. Soc.* **67:** 1135–1138.
21. Lehmler, H-J., M. Jay, and P. M. Bummer. 2000. Mixing of partially fluorinated carboxylic acids and their hydrocarbon analogs with dipalmitoylphosphatidylcholine at the air-water interface. *Langmuir.* **16:** 10161–10166.
22. Lehmler, H-J., M. O. Oyewumi, M. Jay, and P. M. Bummer. 2001. Behavior of partially fluorinated carboxylic acids at the air-water interface. *J. Fluorine Chem.* **107:** 141–146.
23. Lehmler, H-J., and P. M. Bummer. 2002. Mixing of partially fluorinated carboxylic acids with their hydrocarbon analogs at the air-water interface. *J. Colloid Interface Sci.* **249:** 381–387.
24. Lehmler, H-J., and P. M. Bummer. 2004. Mixing of perfluorinated carboxylic acids with dipalmitoylphosphatidylcholine. *Biochim. Biophys. Acta.* **1664:** 141–149.
25. Koynova, R. D., A. I. Boyanov, and B. G. Tenchov. 1987. Gel-state metastability and nature of the azeotropic points in mixtures of saturated phosphatidylcholines and fatty acids. *Biochim. Biophys. Acta.* **903:** 186–196.
26. Eliasz, A. W., D. Chapman, and D. F. Ewing. 1976. Phospholipid phase transitions. Effects of *n*-alcohols, *n*-monocarboxylic acids, phenylalkyl alcohols and quaternary ammonium compounds. *Biochim. Biophys. Acta.* **448:** 220–230.
27. Rohrbaugh, R. H., and P. C. Jurs. 1987. Descriptions of molecular shape applied in studies of structure/activity and structure/property relationships. *Anal. Chim. Acta.* **199:** 99–109.
28. Marsh, D. 1996. Intrinsic curvature in normal and inverted lipid structures and in membranes. *Biophys. J.* **70:** 2248–2255.
29. Albert, A., and E. P. Serjeant. 1962. Ionization Constants of Acids and Bases. A Laboratory Manual. Methuen & Co. Ltd., London.
30. Kellner, B. M. J., F. Müller-Landau, and D. A. Cadenhead. 1978. The temperature-dependence characterization of insoluble films at the air-water interface. *J. Colloid Interface Sci.* **66:** 597–601.
31. Dörfler, H-D. 1990. Mixing behavior of binary insoluble phospholipid monolayers. Analysis of the mixing properties of binary lecithin and cephalin systems by application of several surface and spreading techniques. *Adv. Colloid Interface Sci.* **31:** 1–110.
32. Motomura, K. 1974. Thermodynamics of multicomponent monolayers. I. General formulation. *J. Colloid Interface Sci.* **48:** 307–318.
33. Matuo, H., K. Motomura, and R. Matuura. 1982. Interrelationship between two-dimensional phase diagrams and mean molecular area-mole fraction curves in mixed monolayers. *Chem. Phys. Lipids.* **30:** 353–365.
34. Papahadjopoulos, D. 1968. Surface properties of acidic phospholipids: interaction of monolayers and hydrated liquid crystals with uni- and bi-valent metal ions. *Biochim. Biophys. Acta.* **163:** 240–254.
35. Gaines, G. L. 1966. Insoluble Monolayers at Liquid-Gas Interfaces. Interscience Publishers, New York.
36. Albrecht, O., H. Gruler, and E. Sachmann. 1978. Polymorphism of phospholipid monolayers. *J. Phys.* **39:** 301–313.
37. Helm, C. A., H. Mohwald, K. Kjaer, and J. Als-Nielsen. 1987. Phos-

pholipid monolayers between fluid and solid states. *Biophys. J.* **52:** 381–390.
38. Peterson, I. R., V. Brzezinski, R. M. Kenn, and R. Steitz. 1992. Equivalent states of amphiphilic lamellae. *Langmuir.* **8:** 2995–3002.
39. Bibo, A. M., and I. R. Peterson. 1990. Phase diagrams of monolayers of the long chain fatty acids. *Adv. Mater.* **2:** 309–311.
40. Asgharian, B., D. K. Rice, D. A. Cadenhead, R. N. A. H. Lewis, and R. N. McElhaney. 1989. Monomolecular film behavior of a homologous series of 1,2-bis(ω-cyclohexylacyl)phosphatidylcholines at the air/water interface. *Langmuir.* **5:** 30–34.
41. Balthasar, D. M., D. A. Cadenhead, R. N. A. H. Lewis, and R. N. McElhaney. 1988. Monomolecular film behavior of methyl anteiso-branched-chain phosphatidylcholines. *Langmuir.* **4:** 180–186.
42. Kaganer, V. M., H. Möhwald, and P. Dutta. 1999. Structure and phase transitions in Langmuir monolayers. *Rev. Mod. Phys.* **71:** 779–819.
43. Matuo, H., K. Motomura, and R. Matuura. 1981. Effects of molecular structure on two-dimensional phase diagram and thermodynamic quantities of mixed monolayers. *Chem. Phys. Lipids.* **28:** 385–397.
44. Israelachvili, J. N. 1991. Intermolecular and Surface Forces. Academic Press, San Diego, CA.
45. Israelachvili, J. N., D. J. Mitchell, and B. W. Ninham. 1977. Theory of self-assembly of lipid bilayers and vesicles. *Biochim. Biophys. Acta.* **470:** 185–201.
46. Lohner, K. 1991. Effects of small organic molecules on phospholipid phase transitions. *Chem. Phys. Lipids.* **57:** 341–362.